Available online at www.sciencedirect.com
ScienceDirect
Chemical Physics Letters 444 (2007) 17–22
CHEMICAL PHYSICS LETTERS
www.elsevier.com/locate/cplett

How useful are reactivity indicators for the description of hydrogen abstraction reactions on polycyclic aromatic hydrocarbons?

K. Hemelsoet, V. Van Speybroeck, M. Waroquier *

Center for Molecular Modeling, Ghent University, Proeftuinstraat 86, 9000 Ghent, Belgium

Received 4 January 2007; in final form 20 June 2007
Available online 3 July 2007

Abstract

Hydrogen abstraction reactions at polyaromatic hydrocarbons by a methyl radical are investigated from the viewpoint of DFT-based reactivity descriptors. The BMK functional succeeds in accurately reproducing experimental data for the global indicators. All species are found to be soft. The local HSAB principle shows an overall good qualitative agreement with kinetic barriers, and the local softness is successful for describing the general reactivity trends. However, the indicators do not succeed in predicting the particularly high barriers encountered in some abstraction reactions, as these barriers are mainly caused by steric hindrance effects in the transition structures.

1. Introduction

Polycyclic aromatic hydrocarbons (PAHs) have been intensively studied in modern chemistry [1] as they play an important role in a large number of different areas (e.g. cosmology and combustion chemistry) and as they exhibit carcinogenic characteristics. PAHs are key intermediate products in soot formation and coal conversion processes [2]. More precisely, they can arise from incomplete combustion of organic matter and they are also formed in steam cracking units used in the petroleum industry for the production of light olefines such as ethylene and propylene. In such a reactor the formation of a coke layer – consisting of aromatic rings – on the inner walls of the reactor is observed, reducing the efficiency of the device. In all PAH growth processes, various classes of elementary reactions such as hydrogen abstraction, addition, cyclization and dehydrogenation reactions can be distinguished [3–5]. In a coke network, the initial radical surface species are formed through hydrogen abstraction reactions by small gas phase precursors, such as methyl and hydrogen radicals. Previously, we performed an elaborate level-of-theory study on the hydrogen abstraction reaction at benzene by a methyl radical, representing a reference reaction [6]. We found that the G3-RAD composite procedure, the URCCSD(T), and the cost-effective DFT methods BMK, BB1K and MPW1K give the best results for calculating accurate and reliable thermochemical and kinetic data. Secondly, the study of hydrogen abstraction reactions by a methyl radical has been extended to PAHs, with focus on the influence of the local polyaromatic structure on the thermochemistry and kinetics [7]. Based on kinetic information, we found that abstraction of uncongested hydrogens is preferential, and a normal Bell-Evans-Polanyi relationship was obtained for the series of linear acenes. However, for the more congested locations this was not the case as some large energy barriers were explained in terms of steric hindrance in the transition structures.

Chemical reactivity can also be studied from the viewpoint of DFT-based reactivity indicators. These quantities are response functions, defined as derivatives of the electronic energy functional to the total number of electrons or the external potential [8,9]. In general, studies on indicators of radical species and reactions have so far been limited. Global and local reactivity indicators were calculated for a variety of open-shell systems [10–12]. Radical

* Corresponding author.
E-mail address: michel.waroquier@ugent.be (M. Waroquier).

0009-2614/$ - see front matter © 2007 Elsevier B.V. All rights reserved.
doi:10.1016/j.cplett.2007.06.124

addition reactions [12–14] as well as hydrogen abstraction reactions were most intensively studied [15–17]. Difficulties and shortcomings in the present definitions of radical indicators were already reported [17]. Very recently, a new interest into radical reactions originated with the development of spin–polarized reactivity descriptors and so far, some radical cyclization reactions were already successfully examined [18]. Modelli et al. reported a link between the electron affinity (EA) of PAHs and their toxicity [19]. Some elementary reactions occurring in a coke network were previously studied by the authors, however a limited number of PAHs was tested [20]. Previous works examine the applicability of the reactivity concepts at the qualitative level only. A more quantitative analysis, using the hard–soft acid–base (HSAB) principle, was proposed by Gazquez and Méndez [21] and investigated for various (strong as well as weak) reactions by Pal and coworkers [22,23] and Méndez and coworkers [24,25]. It is however noteworthy to mention that these studies involve typical acid–base complexes, whereas in the present work radical reactions are addressed.

The objectives of this Letter are as follows. First, we assess whether global DFT-based reactivity indicators are capable of providing reliable information about the reactivity sequence of the isolated PAHs. Therefore, a comparison with available experimental data is made. Second, we investigate whether there exists a correlation between various reactivity indicators and reaction barriers and/or enthalpies for hydrogen abstraction. And finally, the applicability of local indicators to describe the correct site-selectivity is examined.

2. Theoretical background

DFT-based reactivity indicators are defined as derivatives of the electronic energy $E[N,v(\mathbf{r})]$ with N the total number of electrons and $v(\mathbf{r})$ the external potential [8,9]. Using the finite difference approach, the chemical potential μ, the global hardness η and global softness S can be computed from the vertical ionization potential (IP) and electron affinity (EA):

$$\mu = -\frac{\mathrm{IP}+\mathrm{EA}}{2}, \quad \eta = \frac{\mathrm{IP}-\mathrm{EA}}{2}, \quad S = \frac{1}{2\eta}. \tag{1}$$

Site-selectivity can be described using local indicators. The Fukui function $f(\mathbf{r})$ and local softness $s(\mathbf{r}) = S\,f(\mathbf{r})$ are predominantly used. The condensed form of $f(\mathbf{r})$ gives an approximate value at the position of an atomic center [26], for a radical attack one obtains:

$$f_k^0 = (q_k(N+1) - q_k(N-1))/2 \tag{2}$$

with $q_k(N)$ the electron population on the kth atom of the molecule with N electrons.

According to the HSAB principle [27] a reaction will be favored when the softness difference is minimal. This rule can be applied on a global level, resulting in reactivity sequences and on a local level, with the additional advantage of distinguishing the preferential site of attack. A semiquantitative version of the HSAB principle was proposed, assuming that a chemical interaction generally consists of two steps [21]. The interaction energy can be written as follows:

$$\begin{aligned}\Delta E_{\mathrm{int}} &= \Delta E_v + \Delta E_\mu \\ &\approx -\frac{1}{2}(\mu_{\mathrm{A}} - \mu_{\mathrm{B}})^2 \frac{S_{\mathrm{A}} S_{\mathrm{B}}}{S_{\mathrm{A}} + S_{\mathrm{B}}} - \frac{1}{2}\frac{\lambda}{S_{\mathrm{A}} + S_{\mathrm{B}}}.\end{aligned} \tag{3}$$

The first step (at constant $v(\mathbf{r})$) corresponds to the equalization of chemical potential, whereas in the second step (at constant μ) the formed complex evolves toward the equilibrium state through changes in the electron density of the global system. The latter is actually a manifestation of the principle of maximum hardness (PMH).

The parameter λ can be related to the participating effective number of valence electrons. For a chemical reaction, the corresponding reaction energy ΔE_{reac} can be written in terms of the ΔE_{int} of the contributing bond breaking and forming reactions [28].

3. Computational details

Full geometry optimizations and frequency calculations for minimum energy and transition state structures were performed within the GAUSSIAN 03 software package [29] using density-functional theory (DFT) with the hybrid B3-LYP functional [30,31] and 6-311G(*d,p*) basis set. Subsequent single-point energy calculations were done using the BMK [32] functional in combination with the large 6-311+G(*3df, 2p*) basis set. The authors previously examined the use of the BMK functional for the computation of global indicators [33]. It is well-known that a proper description of the spatially diffuse electron distributions of anions requires a basis set with diffuse functions. Within this view, Modelli et al. recently showed that inclusion of the smallest addition of diffuse functions is suitable for a correct description of stable PAH anion states and their corresponding EA values [19]. For the local reactivity descriptors, the atomic charges were systematically calculated using the CHELPG scheme [34], which is derived from the electrostatic potential and is known to provide accurate and reliable charges.

4. Results and discussion

In Fig. 1 an overview is given of the PAHs under study. The complete set can be divided into two sub-categories. The first group includes the series of linear acenes (**B**, **N**, **A**, **T** and **P**), while the other group consists of non-linear structures (**PH**, **BPH**, **DBPH**, **BA**, **DBA**, **C**, **BNA**, **BPHA**, **PYR**, **PER** and **BPER**). Hydrogen abstraction reactions at various sites by an approaching methyl radical, resulting in the formation of aryl radicals and methane, are investigated. Throughout the present letter, the notation PAH-X refers to the abstraction of hydrogen atom X from the polycyclic aromatic hydrocarbon PAH.

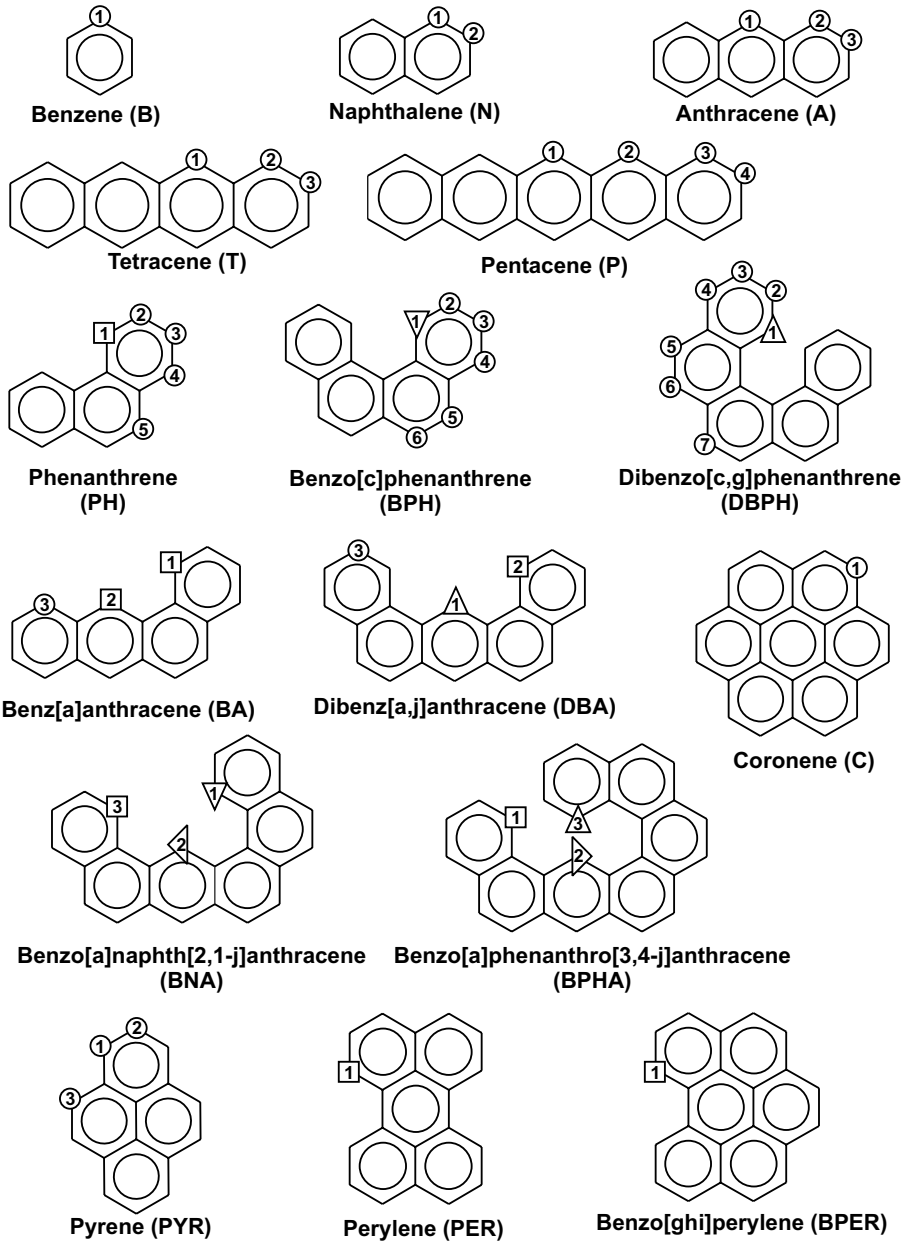

Fig. 1. Structures of polycyclic aromatic hydrocarbons.

Table 1
Vertical electron affinity EA (in eV), chemical potential μ (in eV), global softness S (in au^{-1}) and global electrophilicity ω (in eV) calculated at BMK/6-311+G(*3df, 2p*)//B3-LYP/6-311G(*d, p*) level. Experimental S are given between parentheses

	EA	μ	S	ω		EA	μ	S	ω
B	−1.637	−3.857	2.477 (2.626)	1.354	**BA**	0.400	−3.836	3.959 (3.854)	2.141
N	−0.460	−3.814	3.184 (3.261)	1.702	**DBA**	0.410	−3.849	3.956 (3.996)	2.153
A	0.379	−3.828	3.945 (3.939)	2.125	**BNA**	0.648	−3.848	4.251 (–)	2.313
T	0.974	−3.850	4.731 (4.610)	2.577	**BPHA**	0.657	−3.827	4.293 (–)	2.310
P	1.404	−3.867	5.523 (5.195)	3.035	**C**	0.318	−3.806	3.900 (3.990)	2.077
PH	−0.297	−3.778	3.339 (3.570)	1.752	**PYR**	0.240	−3.786	3.836 (3.929)	2.021
BPH	0.145	−3.833	3.689 (3.720)	1.992	**PER**	0.821	−3.824	4.532 (4.545)	2.435
DBPH	0.220	−3.808	3.792 (–)	2.020	**BPER**	0.577	−3.822	4.192 (4.031)	2.251

The computed EA, μ and S values, as well as experimental softness data (based on vertical IP and EA values) are given in Table 1. The majority of the studied PAHs correspond to energetically favored anion states (EA > 0), the

only exceptions are **B**, **N** and **PH** (EA < 0). In general, all optimized species are considered as soft, since all S values are found in the range between 2.477 and 5.523 au^{-1}. Table 1 also shows that the S values match very well the corresponding experimental values (which are given between parentheses): a linear regression approximation results in an R-squared value of 0.98. The calculated values of **N**, **A**, **BPH**, **DBA**, **C**, **PYR** and **PER** reproduce their experimental counterparts within 0.1 au^{-1} ($\approx$ 0.004 eV^{-1}). The largest discrepancy is noticed for **P**, although the overestimation of the experimental value by 0.3 au^{-1} ($\approx$ 0.01 eV^{-1}) is still limited. This excellent agreement is mainly due to error cancellation between the IP and EA contributions. We note that in the case of negative affinity values (**B**, **N** and **PH**) an alternative formulation proposed by Tozer and De Proft [35] was also used to compute S. The agreement with the experimental values was however not further improved. For the series of linear acenes, it is seen that an increase in molecular size corresponds to an increase of the EA value. In combination with decreasing IP values, this behavior is also observed for S, demonstrating a higher reactivity for the larger linear molecules. It is also seen that the absolute values of the chemical potential of the PAHs (Table 1) are lower than μ of the methyl radical ($\mu = -4.749$ eV), suggesting an electrophilic behavior of the methyl radical. The electrophilicity $\omega(=\frac{\mu^2}{2\eta})$ is a more suitable descriptor to describe this concept and the computed values are therefore tabulated in Table 1. For the methyl radical a value of 2.272 eV was obtained. Based on this information it is clear that the methyl radical can act as an electrophile as well as a nucleophile. This was also reported earlier by Chandra and Nguyen who investigated the addition of the methyl radical to double bonds [17].

Furthermore, the applicability of the global HSAB principle is tested. Therefore, calculated ΔS values – indicating the difference between the global softness of the PAH molecule on one hand and the global softness of the attacking methyl radical ($S = 2.741$ au^{-1}) on the other – are compared with calculated barriers at 0 K (ΔE_0 in kJ mol^{-1}). All computed results are given in Table 2. In a search for a possible correlation between ΔS and the reaction barriers ΔE_0, we plot them in Fig. 2, but there is manifestly no correlation between the two quantities. This could be expected, taking into account the importance of steric effects in several transition structures.

From a semiquantitative point of view, an approximation for the reaction energy of the investigated hydrogen abstractions is calculated using Eq. (3) and the overall results are also included in Table 2. Two contributing radical reactions can be distinguished (as shown in Fig. 3): one bond breaking (splitting of the PAH in an aryl radical and the hydrogen radical, reaction (1)) and one bond forming (between the hydrogen and methyl radical, reaction (2)) reaction are taken into account. Due to the small difference in chemical potentials between the various interacting radicals, the ΔE_v contribution is relatively small compared to the $\Delta E'_\mu$ term (corresponding to $\lambda = 1$). This emphasizes

Table 2
Reaction barrier at 0 K ΔE_0, reaction enthalpy ΔH_{298}, ΔE_v and $\Delta E'_\mu$ (with $\lambda = 1$) as in Eq. (3), all in kJ mol^{-1}, ΔS values in au^{-1} (differences between S of the PAH and the methyl radical with $S = 2.741$ au^{-1})

	ΔE_0	ΔH_{298}	ΔS	ΔE_v	$\Delta E'_\mu$	λ
B-1	71.8	30.6	0.265	0.073	23.570	1.303
N-1	72.7	32.1	0.443	−0.192	34.540	0.923
A-1	74.8	34.3	1.204	−0.063	44.564	0.767
T-1	74.6	34.3	1.990	−0.096	50.029	0.683
P-1	74.4	34.0	2.781	0.054	55.355	0.614
PH-1	76.5	24.7	0.598	−0.523	39.352	0.615
BPH-1	75.2	4.9	0.948	−3.506	47.370	0.030
DBPH-1	74.1	19.3	1.051	−7.071	60.244	0.204
BA-2	82.9	26.8	1.218	−0.458	48.533	0.543
DBA-1	89.2	19.0	1.215	−0.735	52.270	0.350
BNA-2	80.7	−1.8	1.510	−3.440	58.822	0.090
BPHA-2	82.2	12.1	1.551	−6.040	68.777	0.088
C-1	73.2	34.0	1.159	−0.231	48.366	0.699
PYR-2	71.5	30.8	1.095	−0.389	40.446	0.752
PER-1	77.0	23.7	1.791	−0.422	46.396	0.501
BPER-1	76.8	25.9	1.451	−0.266	47.380	0.542

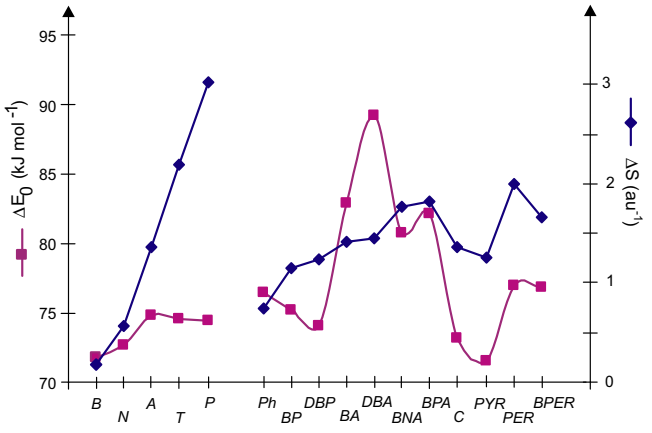

Fig. 2. Global softness differences ΔS (au^{-1}) and energy barriers at 0 K ΔE_0 (kJ mol^{-1}) for hydrogen abstraction reactions at PAHs by a methyl radical.

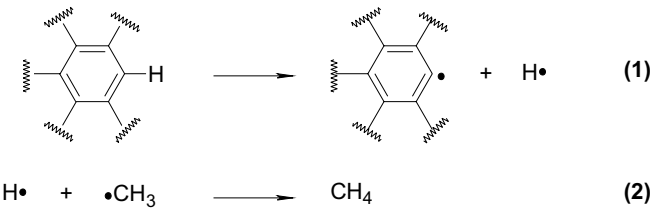

Fig. 3. Contributing radical reactions of the investigated hydrogen abstractions.

the importance of the redistribution of the electron cloud in order to achieve a maximal hardness. For reaction (2) ΔE_v and $\Delta E'_\mu$ equal −8.524 and −276.522 kJ mol^{-1} respectively. For the reactions (1), leading to the various aryl radicals, the ΔE_v contribution lies in the range between −15.6 and −8.4 kJ mol^{-1}, whereas $\Delta E'_\mu$ ranges between − 252.9 and −207.7 kJ mol^{-1}. It is noted that the exact value of λ is difficult to obtain. Moreover, this is often not strictly

necessary within a qualitative discussion of the importance of the separate contributions. However, in literature various methodologies have been proposed to compute the factor λ. Pal and Chandrakumar used the change in the electron densities of the systems before and after the interaction process (in practice, atomic charges were applied) [22]. Méndez et al. explicitly obtained λ values in the case of substituted phenols through a fitting procedure using bond dissociation energies [24]. In the present study, we follow the methodology briefly proposed by Gázquez [28]: a set of λ values are obtained (Table 2) by assuming that the resulting ΔE_{reac} values approximate the reaction enthalpies ΔH_{298} (calculated at BMK/6-311+G(3df,2p)//B3-LYP/6-311G(*d,p*) [7]).

The relatively high values of λ indicate the soft–soft character of the interactions. The scattering of the parameter λ indicates that there is no general correlation between the semiquantitative analysis based on reactivity descriptors and the reaction enthalpies. In previous studies, varying values of λ were also applied, depending on the studied systems [22–25].

While global properties may explain reactivity, site-selectivity is described by local quantities such as the Fukui function and local softness. We investigate, whether these

Table 3
$\Delta s_{C,H_i}$ (in au^{-1}) using the CHELPG scheme. ΔE_0 (in kJ mol^{-1}), scaled ZPVE included, are given in parentheses. Calculated at BMK/6-311+G(*3df, 2p*)//B3-LYP/6-311G(*d,p*) level

i	N	A	T	P	PH
1	2.742 (72.68)	2.810 (74.76)	2.790 (74.57)	2.778 (74.37)	2.758 (76.46)
2	2.673 (71.75)	2.723 (72.60)	2.709 (72.06)	2.777 (74.15)	2.707 (71.55)
3		2.678 (71.29)	2.673 (70.29)	2.705 (71.51)	2.685 (71.97)
4				2.669 (70.79)	2.748 (72.44)
5					2.764 (72.16)
	BPH	**DBPH**	**BA**	**DBA**	**BNA**
1	2.797 (75.22)	2.788 (74.06)	2.744 (76.91)	2.817 (89.17)	2.822 (72.76)
2	2.713 (71.57)	2.731 (71.89)	2.825 (82.88)	2.772 (76.19)	2.896 (80.74)
3	2.710 (72.24)	2.698 (73.01)	2.740 (72.84)	2.740 (71.29)	2.805 (76.55)
4	2.756 (72.77)	2.761 (73.31)			
5	2.727 (73.09)	2.766 (73.67)			
6	2.721 (72.55)	2.732 (72.52)			
7		2.718 (73.84)			
	BPHA	**C**	**PYR**	**PER**	**BPER**
1	2.833 (77.56)	2.730 (73.16)	2.730 (73.33)	2.740 (76.95)	2.745 (76.81)
2	2.962 (82.18)		2.677 (71.50)		
3	2.782 (73.46)		2.760 (71.86)		

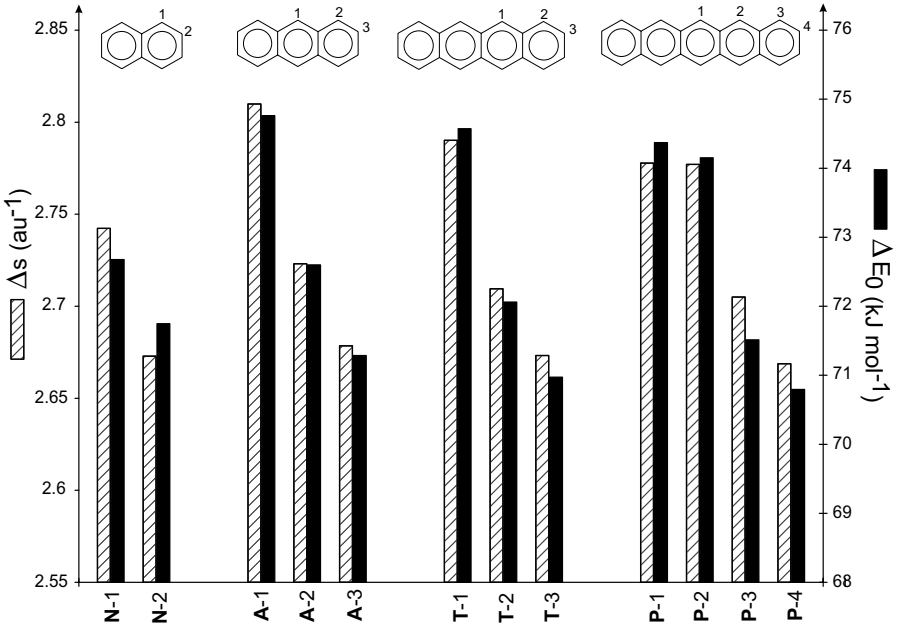

Fig. 4. Local softness differences Δs (au^{-1}) and ΔE_0 (in kJ mol^{-1}) values for the abstraction reactions at various positions in the series of linear acenes.

indicators are able to predict which hydrogen atom is preferred for abstraction. Therefore, softness differences $\Delta s_{C,H_i}$ between the local softness of the carbon atom of the methyl group ($s_C = 2.849\ \text{au}^{-1}$) and the local softness of the various hydrogen atoms of the PAHs are computed (Table 3). The local HSAB principle is hereby investigated from a qualitative viewpoint only, keeping in mind that the global softness values of the reactants differ significantly. The Δs values are scarcely varying for the linear PAHs. The variations are somewhat larger for the non-linear PAHs but still limited to maximum $0.28\ \text{au}^{-1}$. Despite their small differences, we notice a correct correlation between Δs and ΔE_0 for the set of linear acenes. Even the site-selectivity is correctly predicted by the local softness in each linear acene under study, giving preference to a hydrogen abstraction at the outer rings. This behavior is shown in Fig. 4. This correct behavior seems to be also valid for the non-linear series, but there are clearly some pertinent exceptions. For example, in **BNA** the lowest energy barrier is not found at site 3, which corresponds with the lowest Δs. Also for **DBA**-1 the high barrier ($89.17\ \text{kJ mol}^{-1}$, caused by steric hindrance in the transition structure) is not reflected in the local softness value of $2.817\ \text{au}^{-1}$, which globally belongs to the largest values obtained, but is not uniquely the largest one. Summarizing, the local HSAB principle does not work perfectly, and this is probably due to an insufficient incorporation of geometric effects in the transition state, in contrary to the description of the kinetics of the reaction, which contains information of reactant(s), transition state(s) and/or product(s). It is nevertheless important to note that based on local descriptors it is possible to indicate the preferred site of abstraction for most PAHs, as the minimal Δs value corresponds to the minimal ΔE_0 barrier. The condensed local descriptors are found suitable to describe the preferential site of attack, whereas the three-dimensional (not depicted) should be treated with utmost care as these are difficult to interpret.

5. Conclusions

We have critically analyzed the performance of various DFT-based reactivity descriptors. A large set of polyaromatic molecules (PAHs) was tested and the reactivity sequence of the involved species is investigated. The BMK functional in combination with the extended 6-311+G(*3df, 2p*) basis set was used to compute the ionization potential, electron affinity and derived properties such as the chemical potential and global hardness. All PAH molecules are considered as soft and a good agreement with experiment is found. The behavior of the series of linear acenes is highlighted, indicating the increased reactivity for the larger species. It is furthermore also concluded that global hard/soft acid/base considerations can not explain the reactivity of the studied hydrogen abstraction reactions, as the global HSAB principle fails. A semiquantitative approach indicates the importance of the redistribution of the electron cloud in order to achieve a maximal hardness. From a local viewpoint, a good qualitative agreement is obtained between local softness differences and reaction barriers at 0 K. The local softness is well-suited to predict the preferred hydrogen for abstraction by a methyl radical. Due to the fact that the descriptors solely use information of the reactants, none of them succeed in explaining some exceptional high reaction barriers, as these are due to steric hindrance effects in the transition structures.

References

[1] J.M. Gonzales, C.J. Barden, S.T. Brown, P.v.R. Schleyer, H.F. Schaefer III, Q.-S. Li, J. Am. Chem. Soc. 125 (2003) 1064, and references herein.
[2] H. Richter, O.A. Mazyar, R. Sumathi, W.H. Green, J.B. Howard, J.W. Bozzelli, J. Phys. Chem. A 105 (2001) 1561.
[3] M. Frencklach, J. Warnatz, Combust. Sci. Technol. 51 (1987) 265.
[4] S. Wauters, G.B. Marin, Chem. Eng. J. 82 (2001) 267.
[5] L. Vereecken, J. Peeters, H.F. Bettingener, R.I. Kaiser, P.v.R. Schleyer, H.F. Schaefer III, J. Am. Chem. Soc. 124 (2002) 2781.
[6] K. Hemelsoet, D. Moran, V. Van Speybroeck, M. Waroquier, L. Radom, J. Phys. Chem. A 110 (2006) 8942.
[7] K. Hemelsoet, V. Van Speybroeck, D. Moran, G.B. Marin, L. Radom, M. Waroquier, J. Phys. Chem. A 110 (2006) 13624.
[8] R.G. Parr, W. Yang, Density-Functional Theory of Atoms and Molecules, Oxford Science Publications, 1988.
[9] P. Geerlings, F. De Proft, W. Langenaeker, Chem. Rev. 103 (2003) 1793.
[10] R.K. Roy, S. Pal, J. Phys. Chem. 99 (1995) 17822.
[11] G.P. Misra, A.B. Sannigrahi, J. Mol. Struct. (Theochem.) 361 (1996) 63.
[12] A.K. Chandra, M.T. Nguyen, J. Chem. Soc. Perk. Trans. 2 (1997) 1415.
[13] J. Korchowiec, T. Uchimaru, J. Phys. Chem. A 102 (1998) 6682.
[14] H.M.T. Nguyen, J. Peeters, M.T. Nguyen, A.K. Chandra, J. Phys. Chem. A 108 (2004) 484.
[15] A.K. Chandra, T. Uchimaru, M. Sugie, A. Sekiya, Chem. Phys. Lett. 318 (2000) 69.
[16] H.M.T. Nguyen, A.K. Chandra, S.A. Carl, M.T. Nguyen, J. Mol. Struct. (Theochem.) 732 (2005) 219.
[17] A.K. Chandra, M.T. Nguyen, Faraday Discuss. 135 (2007) 191.
[18] B. Pintér et al., J. Org. Chem. 72 (2007) 348.
[19] A. Modelli, L. Mussoni, D. Fabbri, J. Phys. Chem. A 110 (2006) 6482.
[20] K. Hemelsoet, V. Van Speybroeck, G.B. Marin, F. De Proft, P. Geerlings, M. Waroquier, J. Phys. Chem. A 108 (2004) 7281.
[21] J.L. Gázquez, F. Mendéz, J. Phys. Chem. 98 (1994) 4591.
[22] S. Pal, K.R.S. Chandrakumar, J. Am. Chem. Soc. 122 (2000) 4145.
[23] K.R.S. Chandrakumar, S. Pal, J. Phys. Chem. A 106 (2002) 11775.
[24] M.deL. Romero, F. Méndez, J. Phys. Chem. A 107 (2003) 5874.
[25] F. Méndez, J. Tamariz, P. Geerlings, J. Phys. Chem. A 102 (1998) 6292.
[26] W. Yang, W.J. Mortier, J. Am. Chem. Soc. 108 (1986) 5708.
[27] P.W. Ayers, J. Chem. Phys. 122 (2005) 141102, and references herein.
[28] J.L. Gázquez, J. Phys. Chem. A 101 (1997) 9464.
[29] M.J. Frisch et al., Gaussian 03, Revision C.02, Gaussian, Inc., Wallingford, CT, 2004.
[30] A.D. Becke, J. Chem. Phys. 98 (1993) 5648.
[31] C. Lee, W. Yang, R.G. Parr, Phys. Rev. B 37 (1988) 785.
[32] A.D. Boese, J.M.L. Martin, J. Chem. Phys. 121 (2004) 3405.
[33] K. Hemelsoet, D. Lesthaeghe, V. Van Speybroeck, M. Waroquier, J. Chem. Phys. C 111 (2007) 3028.
[34] L.E. Chirlian, M.M. Francl, J. Comp. Chem. 8 (1987) 894.
[35] D.J. Tozer, F. De Proft, J. Phys. Chem. A 109 (2005) 8923.